 

*LIGHT SCATTERING*

PACS numbers: 42.25.Dd; 42.25.Fx; 42.79.Bh
DOI: 10.1070/QE2015v045n08ABEH015741

# 'Photonic jets' from dielectric microaxicons

Yu.E. Geints, A.A. Zemlyanov, E.K. Panina

*Abstract.* **We consider a specific spatially localised light structure, namely, a 'photonic jet' formed in the near field upon scattering of an optical wave in a dielectric micron particle. Dimensional parameters and intensity of a photonic jet from microaxicons of different spatial orientation are studied theoretically. It is found for the first time that an axicon-generated photonic jet has in this case a substantially larger length compared with the case of a jet formed on a spherical particle.**

***Keywords:*** *light scattering, photonic jet, microaxicon.*

## 1. Introduction

The problem of ensuring limiting focusing of optical radiation into a subwavelength-resolution spatial region using light scattering on isolated cylindrical and spheroidal microparticles has been addressed in many papers (see, e.g., review [1]). These studies have been motivated by the fact that laser-illuminated particles having a high degree of spatial symmetry and size on the order of incident light wavelength can produce highly localised light structures, i.e., so-called 'photonic (nano)jets' (PNJs) near the shadow-side surface [2]. Distinctive features of PNJs are an increased (with respect to initial) intensity and spatial dimensions, which are not typical for the case of geometric focusing of light by a conventional collecting lens. The length of a PNJ formed by a micron particle can reach several diameters (tens of wavelengths), and the transverse size can be less than the diffraction limit [3]. In addition, variation of size and optical properties of 'parent' microspheres (i.e., microspheres generating a PNJ) enables controlling PNJ characteristics in a wide range; for example, one can thus increase the PNJ length or intensity [4].

Modern optical technology permit producing miniature objects of more complex geometrical shapes than spheres and ellipsoids, or, for example, microcylinders [5]. Ting [6], Zeng et al. [7] and Pacheco-Pena [8] reported the design of arrays of microprisms, microcones and cubic objects (cuboids), respectively. Each of these diffraction microelements can be used to solve specific practical problems.

Thus, for example, the laser methods for manipulating atoms and molecules, in particular 'laser scissors' and 'laser tweezers', are being actively developed [9, 10]. Their operation principle is based on the effect of occurrence of gradient forces of a light field in the focal waist of the laser beam, so that controlled movement of micro- and nano-objects that fall into the area of optical traps becomes possible. Interestingly, moving the lens focus one can move particles, by arranging them into various structures [11, 12]. It is important here to maximise the length of the regions of optical field focusing in order to be able to directly manipulate a group of target micro-objects.

Traditionally, such a modification of the focal waist of the light beam is realised by axicons or conical lens [13], a characteristic feature of which is specific conical focusing of the incident wave. The spatial structure of the optical field generated by such lenses includes an extended, almost 'diffraction-free' region of the focus, the length of which depends on the vertex (thickness) of the axicon.

Therefore, the idea of applying conical focusing together with the PNJ effect to produce a distributed optical trap of increased length seems promising. Obviously, in this case use should be made of a microcone (microaxicon) rather than a sphere as a parent particle to produce a PNJ. By analogy with the geometrical optics, one can expect that a PNJ generated by a conical micron-size particle will be characterised by a spatial length much greater than the PNJ from the sphere. It is this problem that we study in this paper.

To model the spatial structure of optical fields in the vicinity of microparticles, we used the method of discrete dipole approximation (DDA) [14–16], which allows one, in contrast to the Mie formula [17], to solve the problem of scattering of a light wave from differently shaped objects, and not only from ellipsoids and spheres. Using this technique we have investigated various variants of the PNJ formation from conical particles and have found that the use of a microaxicon with a certain thickness-to-width (vertex angle) ratio gives a dramatic increase in the PNJ length up to values of the order of ten wavelengths of incident light while retaining the subwavelength-resolved transverse size of the photonic jet. A PNJ from a spherical particle with the same cross section is several times shorter.

## 2. DDA method

Let us briefly consider the basic principles and provisions of the DDA method. This method belongs to the family of integrated methods of solving the problem of light scattering on objects. It allows one to find the spatial distribution of the field of a light wave scattered by particles (or a group of particles) according to the known distribution of the optical field inside the scattering object. In fact, the field at any point in

**Yu.E. Geints, A.A. Zemlyanov, E.K. Panina** V.E. Zuev Institute of Atmospheric Optics, Siberian Branch, Russian Academy of Sciences, pl. Akad. Zueva 1, 634021 Tomsk, Russia; e-mail: ygeints@iao.ru

Received 29 December 2014
Kvantovaya Elektronika **45** (8) 743–747 (2015)
Translated by I.A. Ulitkin

space can be represented as the sum of the incident wave field and the field induced by all other elementary segments of the scatterer. These fields interfere and produce the resulting intensity of the scattered wave.

The main difference of the DDA method from its analogues (the method of moments [18], the method of the digitised Green's functions [19]) consists in the fact that during the digitisation procedure of a light scattering object by a given number $N_d$ of elementary polarised segments, they are considered to be electric dipoles, the emission law of which is known. Thus, if the amplitude of the electromagnetic field exciting the dipole is known, we can find the response of this particular dipole and do the same with all the other $N_d$ dipoles. The resulting field will represent a superposition of the external field and the field of all elementary dipoles of the object, taking into account the interaction between the dipoles themselves; therefore, the DDA method is called the coupled dipole method in the literature [20].

Here, following [15], we give a brief mathematical formulation of the DDA method. We consider an object of volume $V$ with the complex refractive index of matter $m = n - i\varkappa$, which in general depends on the spatial coordinates $\boldsymbol{r}$. The real object is replaced by a set $N_d$ of dipoles uniformly distributed in lattice nodes (physical boundaries of the object), the distance between the dipoles being $d$. Each dipole is responsible for polarisability of an elementary part of matter of a scattering particle – a cubic element of volume $d^3$.

Polarisability of each dipole $\alpha_j$ ($j = 1, ..., N_d$) is given in the form of the Clausius–Mossotti relation [21] with the correction for the variance of a discrete lattice of the dipoles in the region of high frequencies ($kd \gg 1$) [22, 23]: $\alpha_j = \alpha_j^{CM}/(1 + D)$, where

$$\alpha_j^{CM} = \frac{3}{4\pi} d^3 \frac{\varepsilon_j - 1}{\varepsilon_j + 2};$$

$$D = \frac{\alpha_j^{CM}}{d^3}\left[\frac{4}{3}(kd)^2 + \frac{2}{3\pi}\ln\left(\frac{\pi - kd}{\pi + kd}\right) + \frac{2}{3}i(kd)^3\right]$$

is the correction factor; $\varepsilon_j$ is the dielectric constant of the material at point $\boldsymbol{r}_j$ of dipole localisation; $k = 2\pi/\lambda$; and $\lambda$ is the wavelength.

The vector of dipole (electric) polarisation is $\boldsymbol{P}_j = \alpha_j \boldsymbol{E}_j$, where

$$\boldsymbol{E}_j = \boldsymbol{E}_j^{inc} - \sum_{l \neq j} A_{lj} \boldsymbol{P}_l \qquad (1)$$

is the resultant field at point $\boldsymbol{r}_j$ inside the object, consisting of the incident wave field $\boldsymbol{E}_j^{inc} = \boldsymbol{E}_0 \exp(i\boldsymbol{k}\boldsymbol{r}_j - i\omega t)$ and the contribution of each of the remaining $N_d - 1$ dipoles; $\boldsymbol{k}$ is the wave vector in the direction of propagation of an electromagnetic wave ($k = |\boldsymbol{k}| = \omega/c$); and $\sum_{l \neq j} A_{lj} P_l$ is the electric field at point $\boldsymbol{r}_j$ of emission of a dipole with polarisation $\boldsymbol{P}_l$, located at the points $\boldsymbol{r}_l$, taking into account its delay while propagating a distance $r_{jl} = |\boldsymbol{r}_j - \boldsymbol{r}_l|$.

Each element $A_{lj}$ is a third-order square matrix:

$$A_{lj} = \frac{\exp(ikr_{jl})}{r_{jl}}\left[k^2(\tilde{r}_{jl}\tilde{r}_{jl} - I_3) + \frac{ikr_{jl} - 1}{r_{jl}^2}(3\tilde{r}_{jl}\tilde{r}_{jl} - I_3)\right], \; l \neq j,$$

where $\tilde{r}_{jl} = (\boldsymbol{r}_j - \boldsymbol{r}_l)/r_{jl}$, and $I_3$ is the $3 \times 3$ unit matrix. The diagonal elements of the matrix $\hat{A}$ are written through the polarisation dipoles at point $\boldsymbol{r}_j$: $A_{jj} = 1/\alpha_j$. The further procedure is to find the set of polarisations $\boldsymbol{P}_l$ by solving the system of $3N_d$ linear equations (in the complex plane):

$$\sum_{l=1}^{N_d} A_{lj} \boldsymbol{P}_l = \boldsymbol{E}_j^{inc}. \qquad (2)$$

Then we can calculate the amplitude of the optical field of the scattered wave:

$$\boldsymbol{E}_{sc}(\boldsymbol{r}) = \frac{k^2 \exp(ikr)}{r} \sum_{j=1}^{N_d} \exp(-ik\tilde{r}\boldsymbol{r}_j)(\tilde{\hat{r}}\tilde{\hat{r}} - I_3)\boldsymbol{P}_j. \qquad (3)$$

The total field outside of the particle is the sum of the fields of the incident and scattered waves: $\boldsymbol{E}(\boldsymbol{r}) = \boldsymbol{E}^{inc}(\boldsymbol{r}) + \boldsymbol{E}_{sc}(\boldsymbol{r})$, and thus, taking (1) into account the problem of light scattering can be considered solved.

In carrying out numerical calculations, we used a freely available open-source DDSCAT software package designed by Draine and Flatau [15]. The latest version of the Fortran-90 source code, as well as documentation and examples can be downloaded from http://code.google.com/p/ddscat/. Based on the objectives set in the work, we have made some changes in the source code of the DDSCAT package, modifying the presentation unit of output results and adding the procedures generating an array of spatial points occupied by the dipoles for a truncated cone with different orientation and a cone connected to the hemispherical lens.

## 3. Characteristics of a PNJ from conical microparticles

Effect of the PNJ formation is shown in Fig. 1a, which presents a two-dimensional distribution of the relative laser light intensity $B = I(y,z)/I_0$ ($I_0$ is the intensity of the incident light wave) in the vicinity of a homogeneous spherical particle of radius $a_0 = 1$ μm. Hereafter, for definiteness, we consider silica nonabsorbing particles (with a real refractive index $n = 1.5$) located in the air and illuminated by laser light at $\lambda = 0.532$ μm.

We have considered two main types of particles: a sphere and an axicon. In the latter case (Figs 1b, 1c), the microparticle orientation with respect to the incident light was changed since we expected that it entails a change in the focusing properties of the microcone associated with different deformation of the wave front of the light incident on the particle, and as a result, the characteristics of field in the PNJ region.

To investigate and compare PNJs from different particles, we select, according to [3], three main parameters: the effective length $L$, the transverse dimension $R$ and the peak intensity $B_{max}$. We will also take into account the distance $h$ of the PNJ from the surface of microparticles. These characteristics are defined in Fig. 1c while considering the spatial intensity profiles of the optical field in the external focus of a quartz axicon. The longitudinal profile is given by the cross section of the two-dimensional distribution $B(y,z)$ of the straight line $y = 0$, and the transverse profile – by the cross section of the straight line parallel to the $y$ axis and passing through the point corresponding to the absolute intensity maximum $B_{max}$ in the PNJ. The longitudinal width of the main peak obtained at the $1/e^2$ level is taken to be the PNJ length $L$. Similarly, we determine the characteristic half-width $R$ of the photon flux.

Analysis of Figs 1a–c shows that by changing the form and/or orientation of the parent particle, one can change the characteristics of the light field in the PNJ region. This high sensitivity of the PNJ spatial form and intensity to a change of the type and size of a light scattering particle (as well as its opti-

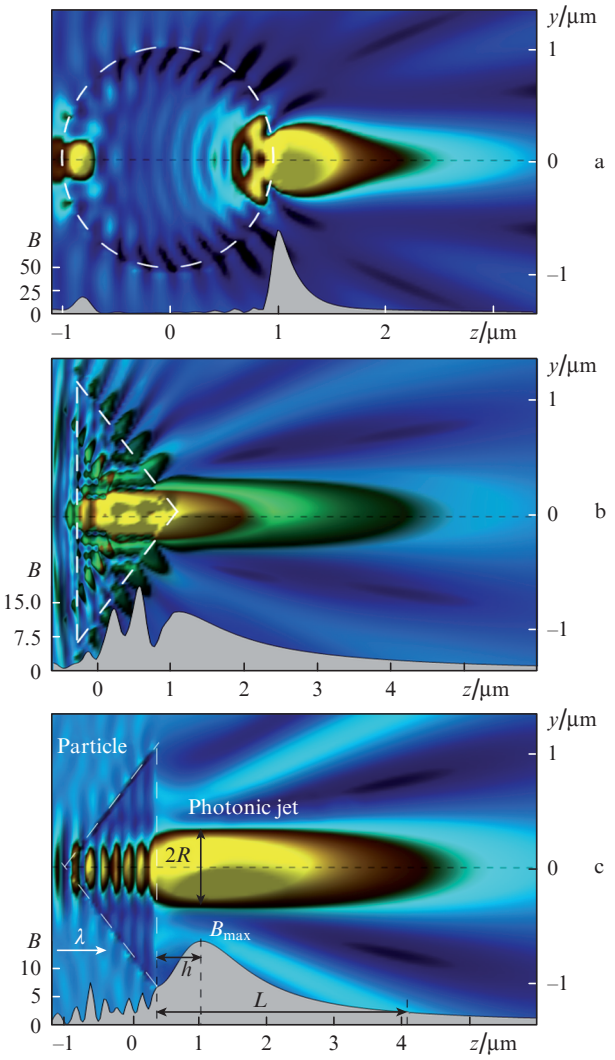


**Figure 1.** Tone distributions of the relative optical-field intensity $B(y,z)$ in the vicinity of quartz particles illuminated with laser light at $\lambda$ = 0.523 μm for a sphere of radius $a_0$ = 1 μm (a) and a microaxicon with a base diameter $D_a$ = 2 μm and thickness $L_a = D_a/2$ at its different orientations (b, c). The radiation is incident from the left. Here and in Figs 2 and 3 lower parts of each figure present the distribution cross section at $y = 0$.

cal properties) allows the PNJ parameters to be effectively manipulated [3]. Consider how the PNJ form is modified when the sphere is replaced by an axicon with equal cross section.

As a rule, in optical beam-shaping systems the axicon is illuminated by laser light from its base. In the case of a microcone, in this configuration (as shown in Fig. 1b) the optical field is localised mainly inside the axicon ($B \sim 17$) and the 'flowing' light flux (PNJ) of length $L \approx 5\lambda$ has a lower intensity ($B_{max} \approx 11$). In the case of mirror configuration of the microcone ('inverse' axicon), as shown in Fig. 1c, the position of the intensity maximum of the photon flux moves away from the particle ($h \approx 2\lambda$), which is visually perceived as a separation of the jet from the particle surface. Numerical estimates have shown that, although this spatial orientation of the axicon particle has no significant gain in intensity compared to the traditional position of the axicon, this can significantly increase the length of the generated PNJ.

Since the objective of the present study was to find microobjects capable of generating extended PNJs, below we consider the inverse axicon (see Fig. 1c) and examine in more detail the main PNJ characteristics by varying its size parameters.

First of all, we will show how the change in the microaxicon thickness influences the characteristics of the optical field near the surface of its shadow side (the PNJ region). As an example, we consider two variants, when the cone thickness $L_a$ constituted a quarter of the diameter of its base $D_a$ ($L_a = D_a/4$) or is equal to the diameter ($L_a = D_a$). When the Da value is fixed, it actually corresponds to a change in the vertex angle of the axicon.

From a series of two-dimensional intensity distributions of the field, presented in Fig. 2, one can see that a decrease in the thickness of the focusing particle leads to a drastic increase in the length of the photon flux outside of the particle (Fig. 2a). However, this effect is accompanied by a more than two-fold decrease in peak intensity of the PNJ ($B_{max}$ = 6.2) and by a 1.5-fold increase in its transverse size in comparison with the case of a wider axicon (Fig. 2b). Thus, for a short axicon ($L_a = D_a/4$), we have $L \approx 10\lambda$ and $R \approx \lambda$. At the same time, for a wider particle these characteristics are respectively $\sim 6\lambda$ and $\sim 0.75\lambda$. It should be noted that for a spherical particles with the same transverse cross section the main PNJ parameters are as follows: $B_{max} = 84$, $L = 0.85\lambda$, $R = 0.68\lambda$.

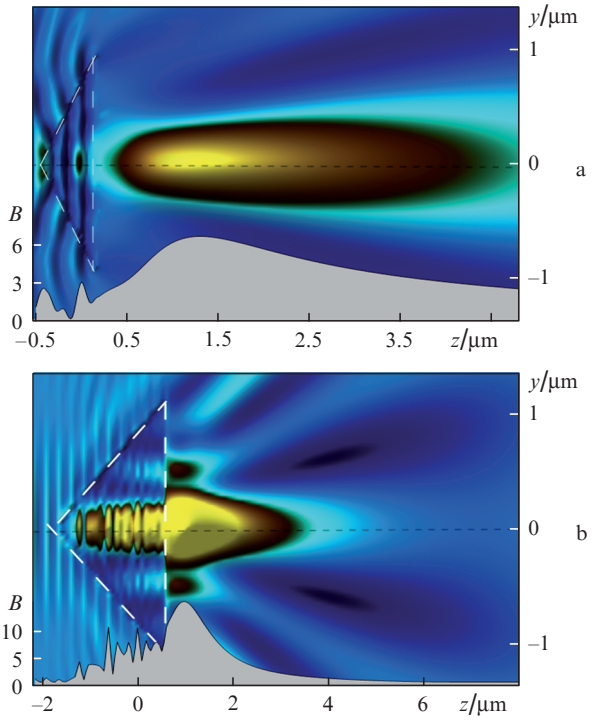


**Figure 2.** PNJ from axicon particles with the base diameter $D_a$ = 2 μm and thickness $L_a$ = (a) $D_a/4$ and (b) $D_a$.

The use of an axicon, as clearly demonstrated above, results in abnormally extended photonic jets; however, their transverse size is greater than that of the PNJ from the sphere, and the intensity is less. However, a number of optical applications related to micro-machined holes [7, 24], control of micro- and nanoparticles [25, 26] require generation of extended high-intensity submicron jets with the transverse size, approaching the diffraction limit: $R \sim \lambda/2$. Consequently, there appears a problem of increasing the spatial resolution of

the PNJ from the axicon particle while retaining as much as possible, its length. This causes the search for the other types of particles, for which the focusing region has a sufficiently good spatial localisation at high intensity.

To solve this problem, we propose to construct a combined particle consisting of a cone and a hemisphere. The basic idea here is to use the advantages of the conical (length) and spherical (high intensity) focusing of the light wave. As a basic particle we will choose a circular cone, inheriting the ability of an axicon to form long PNJs. The addition of the hemisphere at the output section of the cone will allow for additional focusing adjustment of incident light, which should increase the peak intensity of the PNJ and reduce its width.

Tone distributions of the relative laser light intensity $B$ in the vicinity of combined axisymmetric quartz microparticles with a radius $a_0 = 1$ μm of the base of the truncated axicon is shown in Fig. 3. As in previous figures, the intensity is normalised to the maximum value. Axicon thicknesses correspond to the cases shown in Figs 1 and 2.

The qualitative comparison of Figs 2 and 3 shows how the field distribution changes inside and outside of the particle when the axicon is combined with the sphere. The PNJ length becomes several times less as compared to the case of light scattering from an ideal axicon. Moreover, not only the spatial size of the PNJ, but also its distance from the surface change. The jet as if 'sticks' to the outer shell of the complex particle, 'leaking' out of it in the form of an exponentially decaying tail. According to the terminology adopted in [27], for the combined particle the morphological type of the PNJ changes from a torch, as in Fig. 2a, to a dagger. However, the overall trend noted previously in Fig. 2 is retained, i.e., the length of the photon flux outside of the particle decreases with increasing axicon thickness.

The dependences of the main characteristics of the PNJ on the axicon thickness for conical and combined particles are shown in Fig. 4. One can see that among the studied particles axicons with a ratio of dimensional parameters $L_a = D_a/4$ generate the longest photonic jet. In this case, the peak intensity of the PNJ is almost an order of magnitude higher than the incident light intensity, and the transverse size of the jet is on the order of the wavelength of light ($R \sim \lambda$). For the cones with the greatest (of variants considered) thickness the maximum PNJ intensity is reached, and the half-width of the jet has a minimum size ($R \sim 0.66\lambda$).

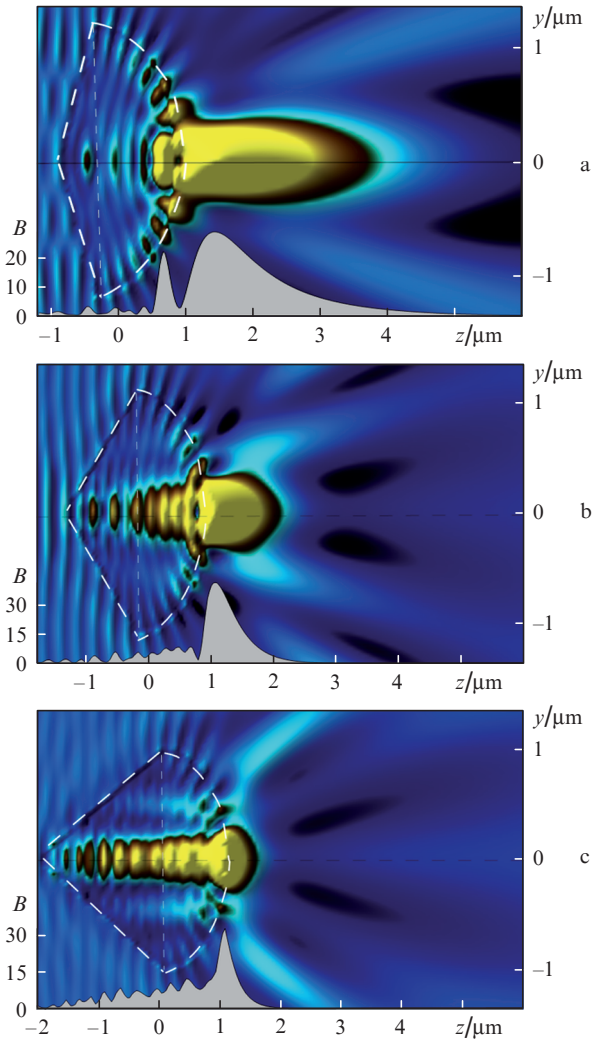


**Figure 3.** Same as in Fig. 2 for the combined particles with $L_a$= (a) $D_a/4$, (b) $D_a/2$ and (c) $D_a$.

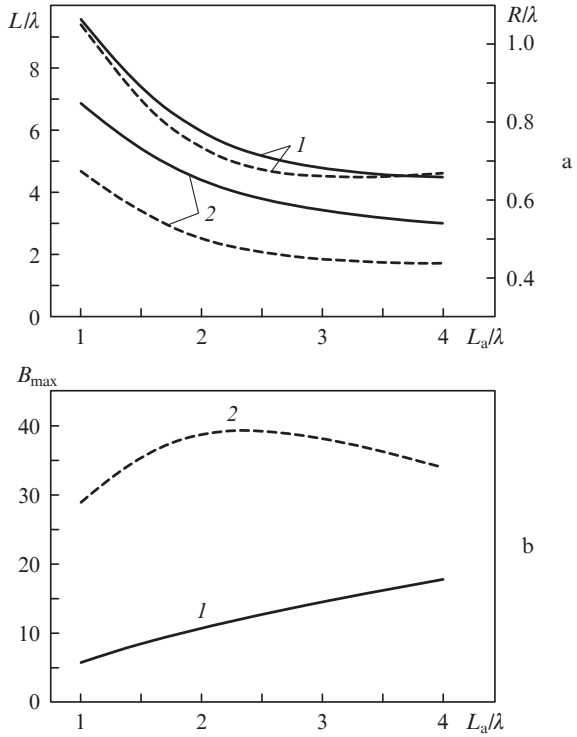


**Figure 4.** Parameters of a PNJ from (*1*) a microaxicon and (*2*) a combined particles as a function of the axicon thickness: (a) the PNJ length $L$ (dashed curves) and the width $R$ (solid lines), as well as (b) the maximum intensity $B_{max}$.

In combined axicon + hemisphere particles, the PNJ length does not change much when the length of the axicon is varied, and the half-width of the jet is stabilised at the subwavelength level: $R \sim \lambda/2$. The additional spherical focusing, achieved due to the attachment to the hemisphere axicon, allows one to have a more than three-fold increase in the intensity near the shadow-side surface of the microparticle.

Overall assessment of the PNJ parameters can be carried out using the quality criterion $Q$, which takes into account all the characteristics of the jet: $Q = LB_{max}/R$ [28]. Figure 5 shows

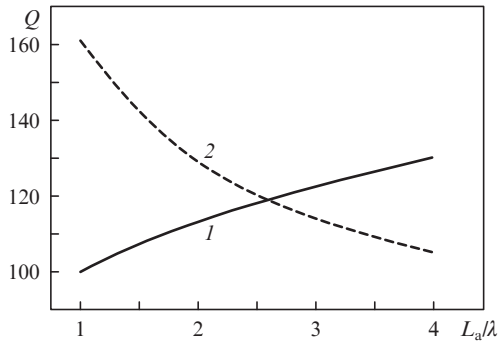


**Figure 5.** Dependences of the PNJ quality criterion $Q$ for (*1*) an axicon and (*2*) a combined particle on the axicon thickness.

the dependences of this parameter on the thickness $L_a$, calculated for axicon particles in the presence or absence of the hemisphere on the right. Note that the value of the quality criterion $Q$ for a uniform spherical particle of the same radius is 106.

One can see from Fig. 5 that an increase in axicon length leads to an increase in the parameter $Q$, primarily due to spatial localisation of the PNJ (a decrease in its transverse size) and an increase in intensity. Comparison with the sphere suggests that in terms of the PNJ quality criteria the conical particle is, of course, an attractive object for generating extended spatially localised light fluxes. The combined use of conical and spherical focusings gives an additional gain in the value of $Q$ for the combined particles having a thickness of $L_a \leqslant D_a/2$.

## 4. Conclusions

The above examples of diffraction structures generated in the near-field due to scattering of light on quartz dielectric uniform microparticles in the form of the right and inverse axicon, as well as in the form of combined particles (axicon + hemisphere) indicate the difference between the spatial forms of PNJs. Implementation of conical focusing on axicons allows localisation of the optical fields into abnormally extended regions. A kind of advantage for the increased length is lower peak intensity and larger width of the photon flux compared with the case of spherical particles.

More advantageous in terms of improving the power characteristics of PNJs are combined particles, representing an inverse axicon supplemented with a hemisphere on the right. The spherical surface allows tighter focusing of the optical field, which results in a several-fold intensity increase in the PNJ region and is always accompanied by a decrease in the jet length. The transverse size of these light fluxes is $\sim\lambda/2$.

Thus, we have clearly demonstrated that by varying the spatial form of light-scattering microaxicons one can control the characteristics of photonic jets by increasing their length or intensity.

## References


1. Heifetz A., Kong S.-C., Sahakiana A.V., Taflove A., Backman V. *J. Comput. Theor. Nanosci.*, **6** (9), 1979 (2009).
2. Chen Z., Taflove A., Backman V. *Opt. Express*, **12** (7), 1214 (2004).
3. Geints Yu.E., Panina E.K., Zemlyanov A.A. *Opt. Commun.*, **283**, 4775 (2010).
4. Geints Yu.E., Panina E.K., Zemlyanov A.A. *J. Opt. Soc. Am. B*, **28** (8), 1825 (2011).
5. Fang Z., Dai T., Zhang B., Zhu X. *Proc. SPIE Int. Soc. Opt. Eng.*, **6831**, 683102 (2008), DOI: 10.1117/12.767590.
6. Ting D.Z.-Y. *Proc. SPIE Int. Soc. Opt. Eng.*, **4992**, 43 (2003), DOI: 10.1117/12.475711.
7. Zeng D., Latham W.P., Kar A. *Opt. Eng.*, **45** (9), 094302 (2006), DOI: 10.1117/1.2353119.
8. Pacheco-Pena V., Beruete M., Minin I.V., Minin O.V. *Appl. Phys. Lett.*, **105**, 084102 (2014), DOI: 10.1063/1.4894243.
9. Astratov V.N., Darafsheh A., Kerr M.D., Allen K.W., Fried N.M., Antoszyk A.N., Ying H.S. *SPIE Newsroom*, **12**, 32 (2010).
10. Garces-Chavez V., McGloin D., Melville H., Sibbett W., Dholakia K. *Nature*, **419**, 145 (2002).
11. Kawata S., Sugiura T. *Opt. Lett.*, **17**, 772 (1992).
12. Taguchi K., Ueno H., Hiramatsu T., Ikeda M. *Electron. Lett.*, **33**, 413 (1997).
13. Liberale C., Mohanty S.K., Mohanty K.S., Degiorgioa V., Cabrinid S., Carpentierod A., Ferrarid E., Cojoc D., Fabrizio E.D. *Proc. SPIE Int. Soc. Opt. Eng.*, **6095**, 1605 (2006), DOI: 10.1117/12.647277.
14. Purcell E.M., Pennypacker C.R. *Astrophys. J.*, **186**, 705 (1973).
15. Draine B.T., Flatau P.J. *J. Opt. Soc. Am. A,* **11**, 1491 (1994).
16. Draine B.T., Flatau P.J. *J. Opt. Soc. Am. A,* **25**, 2693 (2008).
17. Bohren C.F., Hoffman D.R. *Absorption and Scattering of Light by Small Particles* (New York: Wiley, 1983; Moscow: Mir, 1986).
18. Harrington R. *IEEE Antennas Propag. Mag.*, **32** (3), 31 (1990).
19. Goedecke G.H., O'Brien S.G. *Appl. Opt.*, **27**, 2431 (1988).
20. Singham S.B., Bohren C.F. *Opt. Lett.*, **12**, 10 (1987).
21. Born M., Wolf E. *Principles of Optics* (London: Pergamon, 1970; Moscow: Nauka, 1973).
22. Draine B.T., Goodman J. *Astrophys. J.*, **405**, 685 (1993).
23. Gay-Balmaz P., Martin O.J.F. *Comput. Phys. Commun.*, **144**, 111 (2002).
24. Munzer H.J., Mosbacher M., Bertsch M., Zimmermann J., Leiderer P., Boneberg J. *J. Microsc.*, **202**, 129 (2001).
25. Li X., Chen Z., Taflove A., Backman V. *Opt. Express*, **13** (22), 526 (2005).
26. Heifetz A., Simpson J.J., Kong S.-C., Taflove A., Backman V. *Opt. Express*, **15** (25), 17334 (2007).
27. Geints Yu.E., Panina E.K., Zemlyanov A.A. *Opt. Atmos. Okeana*, **25** (5), 417 (2012).
28. Kong S.-C., Taflove A., Backman V. *Opt. Express*, **17** (5), 3722 (2009).